

Conformations of Perfluoropoly(oxyethylene) from Ab Initio Electronic Structure Calculations on Model Molecules

Grant D. Smith¹

Thermosciences Institute, STC 230-3 NASA Ames Research Center,
Moffett Field, California 94035

Richard L. Jaffe

NASA Ames Research Center, Moffett Field, California 94035

Do Y. Yoon*

IBM Research Division, Almaden Research Center, 650 Harry Road,
San Jose, California 95120

Received January 17, 1995; Revised Manuscript Received May 3, 1995*

ABSTRACT: The conformational characteristics of perfluoropoly(oxyethylene) (PFPOE) chains have been investigated in detail, based upon ab initio electronic structure calculations on the model molecules perfluorodiethyl ether and perfluoro-1,2-dimethoxyethane, and have also been compared with those of poly(oxyethylene) (POE) and poly(tetrafluoroethylene) (PTFE). The C-C-O-C bond exhibits split trans conformations, similar to those for the C-C-C-C bond in PTFE, which are strongly favored over the gauche state by 2.5 kcal/mol. In contrast, O-C-C-O bond shows no splitting for the trans or gauche conformations due to the absence of pendant fluorine atoms on the oxygen atoms, and favors a gauche conformation over the trans state by about 0.2 kcal/mol, according to MP2 level ab initio calculations using a D95+* basis set. This oxygen gauche effect, coupled with an expanded C-O-C skeletal angle of 122°, results in a relatively small predicted random coil dimension for PFPOE with a characteristic ratio of $C_\infty \approx 3.9$ at 300 K. Within the limits of ab initio values for the conformational energies and geometries, the predicted value is in good agreement with experimental results of about 4.9.

Introduction

Perfluoropolyethers (PFPE's) form a class of technologically important polymers used widely in a variety of tribological applications because of their low glass transition temperatures, low surface energies, wide temperature range of useful viscosities, low volatilities, and good chemical and thermal stabilities. Despite their wide use as lubricants in applications as varied as jet turbines and magnetic disks for information storage, the molecular level origin of these properties of PFPE's is not well understood. Very recent light scattering and viscometric studies² indicate that PFPE's are conformationally very flexible, with random coil dimensions at room temperature which are much more compact than those of poly(tetrafluoroethylene) (PTFE) at 600 K.³

In an effort to gain a better understanding of the conformational properties of PFPE's, we have performed extensive ab initio electronic structure investigations of the geometries and conformational energetics of a series of perfluoroethers (PFE's) whose structures represent repeat units of various PFPE's. We have utilized the conformational characteristics of the model molecules obtained from the ab initio calculations to parameterize rotational isomeric state (RIS) models for the polymers. In this paper we report on our study of perfluoropoly(oxyethylene) (PFPOE). The chemical structures of PFPOE and its model molecules are shown in Figure 1. Here, we compare RIS predictions of chain dimensions of PFPOE with recent experimental data. The conformational energetics of the model compounds and RIS predictions for properties of PFPOE are also compared with similar calculations on alkyl ether analogs. In future papers we will present results for other perfluoropoly(alkyl ethers).

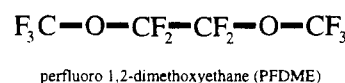
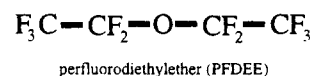
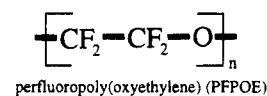


Figure 1. Structure of perfluoropoly(oxyethylene) and its model molecules.

Ab Initio Calculations

Quantum chemistry calculations were performed to determine the geometries and energies of the low-energy conformations of the model molecules shown in Figure 1. These calculations were performed in a manner similar to that used previously in studies of perfluoroalkanes⁴ and alkyl ethers.^{5,6} Initial geometry optimizations were performed at the SCF level using a 4-31G basis set employing the computational chemistry code GRADSCF.⁷ Calculations of the harmonic normal mode vibrational frequencies at this level allowed us to determine which conformations correspond to local energy minima or saddle points and provided starting geometries for subsequent calculations using a larger basis set. These calculations, including geometry optimizations, were carried out using a D95+* basis set, a Dunning⁸ double- ζ basis set with diffuse and polarization functions on all atoms. The inclusion of diffuse functions is important in polar molecules, while polarization functions are required for an accurate description of dispersion interactions. (The exponents for the

* Abstract published in *Advance ACS Abstracts*, July 15, 1995.

Table 1. Conformations of PFB and *n*-Butane

conf	molecule ^a	geometry ^b ϕ_1 cccc	energy ^c			
			SCF		MP2	
			4-31G	D95+*	4-31G	D95+* 6-311G(2df,p)
<i>t</i> ₊	PFB	13.5	0.00	0.00	0.00	0.00
<i>t</i>	<i>n</i> -butane	0.00				0.00
<i>g</i> ⁺	PFB	124.4	1.73	1.02	1.15	0.47
<i>g</i> ⁺	PFB	84.8	2.06	1.94	1.70	1.71
<i>g</i> ⁺	<i>n</i> -butane	117.2				0.53

^a *n*-Butane entries are italicized. ^b PFB geometries were optimized at the SCF level using a D95+* basis set.⁴ *n*-Butane geometries were optimized at the MP2 level using a 6-311G(2df,p) basis set.¹¹ ^c Relative to the *t*₊ for the PFB and the *t* conformer for *n*-butane, in kcal/mol.

diffuse and polarization functions are given in Table 2.) The larger basis set geometry optimizations were performed using the computational chemistry code TURBOMOL.⁹ All D95+* calculations were performed using the TURBOMOL⁹ contraction of the D95 basis set. Electron correlation effects were considered by performing MP2 level calculations using the 4-31G and D95+* basis sets with the respective SCF optimized geometries. The MP2 level calculations for the larger basis set were performed using the computational chemistry code GAUSSIAN92.¹⁰ All calculations were performed on IBM RS/6000 workstations and a Cray C90 at the NASA Ames Research Center.

Perfluoroalkanes. Previously, we considered the influence of fluorine atoms on the conformations of *n*-perfluoroalkanes by comparing the conformational characteristics of perfluoroalkanes with those of *n*-alkanes. The geometries and energies of the low-energy conformers of perfluorobutane⁴ and *n*-butane¹¹ are shown in Table 1. Replacement of the relatively small hydrogen atoms with the larger fluorine atoms results in a much higher degree of steric crowding. To relieve this crowding, each trans (*t*) or gauche (*g*) conformation in perfluorobutane splits to form *t*₊, *t*₋, *g*⁺, (*g*⁻), and *g*⁺ (*g*⁻) conformations. These split conformations allow for interdigitation of the atoms, thereby partially alleviating steric crowding at the expense of distorting the torsional angles.⁴ The larger distortion of the torsional angle for the *g*⁺ conformation, relative to the *g*⁺ conformation, accounts for the higher energy of this conformation.

Perfluoroethers. The PFE molecules studied as model molecules for PFPOE are illustrated in Figure 1. In this section the conformational geometries and

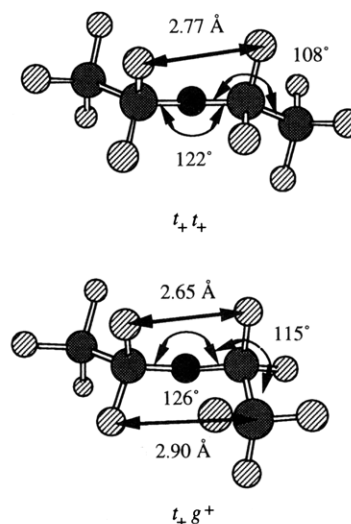


Figure 2. Geometries of low-energy conformations of perfluorodiethyl ether.

energies for the important conformers of the model molecules, as determined from ab initio electronic structure calculations, are presented. The conformational characteristics are compared with results from our previous studies of analogous alkyl ethers. The parameterization of a RIS model for PFPOE based upon the conformational energetics of the model PFE molecules is presented in the next section.

Perfluorodiethyl Ether (PFDEE). The conformational energies and geometries of the important conformations of PFDEE are given in Table 2. The C-C-O-C trans conformation in PFDEE splits into *t*₊ and *t*₋ conformations, as was found for the C-C-C-C trans conformation in perfluoroalkanes (Table 1). The PFDEE *t*₊*t*₊ conformer, illustrated in Figure 2, is the lowest energy conformer. As was found for perfluoropentane,⁴ the *t*₊*t*₋ conformation is not a stationary point. In contrast to DEE,⁵ where the *tt* conformer was found to be of the lowest energy, the *tt* conformation in PFDEE is a saddle point between the *t*₊*t*₊ and *t*₋*t*₋ conformers. The next lowest energy PFDEE conformer is the *t*₊*g*⁺ conformer, also illustrated in Figure 2. The C-C-O-C gauche conformation in PFDEE does not split, in contrast to perfluoroalkanes, where splitting of the C-C-C-C gauche conformation is seen. The lack of splitting of the C-C-O-C gauche conformation in PFDEE can be understood in terms of steric crowding

Table 2. Conformations of PFDEE and DEE

conf	molecule ^a	type ^b	geometry ^c		energy ^d				
			ϕ_1 cc-oc	ϕ_2 co-cc	SCF		MP2		
					4-31G	D95*	4-31G	D95+*	D95+(2df,p)
<i>t</i> ₊ <i>t</i> ₊	PFDEE	min	18.8	18.8	0.00	0.00	0.00	0.00	
<i>tt</i>	PFDEE	sp	0.0	0.0	0.32	0.55	0.46	0.87	
<i>t</i> ₊ <i>t</i> ₋	PFDEE	ns							
<i>tt</i>	DEE	min	0.0	0.0					0.0
<i>t</i> ₊ <i>g</i> ⁺	PFDEE	min	20.9	117.1	3.68	3.50	3.20	2.54	
<i>t</i> ₊ <i>g</i> ⁻	PFDEE	ns							
<i>tg</i> ⁺	DEE	min	5.1	102.0					1.45
<i>g</i> ⁺ <i>g</i> ⁺	PFDEE	min	117.3	117.3	8.41	7.45	7.45	5.54	
<i>g</i> ⁺ <i>g</i> ⁻	DEE	min	91.6	91.6					2.94
<i>g</i> ⁺ <i>g</i> ⁻	PFDEE	ns							
<i>g</i> ⁺ <i>g</i> ⁻	DEE	sp	85.8	-86.1					4.08

^a Alkyl ether entries are italicized. ^b min = local minimum, sp = saddle point, ns = not stationary. ^c Perfluoroalkyl ether geometries are from D95+* SCF optimizations. Alkyl ether geometries are from D95** SCF optimizations. ^d Relative to the *t*₊*t*₊ conformer of PFDEE or the *tt* conformer of DEE. For perfluoroalkyl ethers, diffuse and polarization exponents were as follows: For C, $\alpha_s = 0.0511$, $\alpha_p = 0.0382$, $\alpha_d = 0.75$. For O, $\alpha_s = 0.0949$, $\alpha_p = 0.0712$, $\alpha_d = 0.85$. For F, $\alpha_s = 0.1211$, $\alpha_p = 0.0911$, $\alpha_d = 0.90$. See refs 5 and 6 for alkyl ethers.

Table 3. Conformations of PFDME and DME

conf	molecule ^a	type	geometry ^b			energy ^c				
			ϕ_1 co-cc	ϕ_2 oc-co	ϕ_3 cc-oc	SCF		MP2		
						4-31G	D95+*	4-31G	D95+*	D95+(2df,P)
<i>t+tt+</i>	PFDME	min	18.7	2.1	18.7	0.00	0.00	0.00	0.00	
<i>t+tt-</i>	PFDME	min	18.5	0.0	-18.5	-0.03	-0.02	-0.01	0.00	
<i>ttt</i>	PFDME	sp	0.0	0.0	0.0	0.53	0.93	0.86	1.56	
<i>ttt</i>	DME	min	0.0	0.0	0.0					0.0
<i>t+g+t+</i>	PFDME	min	18.3	121.2	18.3	-0.16	-0.08	-0.48	-0.21	
<i>t+g-t+</i>	PFDME	min	18.2	-116.9	18.2	-0.32	-0.14	-0.49	-0.31	
<i>t+g+t-</i>	PFDME	min	19.0	119.3	-18.5	-0.26	-0.13	-0.50	-0.32	
<i>tg+t</i>	PFDME	sp	-0.4 ^d	117.8	-0.4	0.30		0.36		
<i>tg+t</i>	DME	min	-4.7	106.4	-4.7					0.14
<i>t+tg-</i>	PFDME	min	15.3 ^d	-1.8	-105.2	3.80		3.29		
<i>t+tg+</i>	PFDME	min	14.7 ^d	-3.0	106.1	3.91		3.40		
<i>ttg+</i>	DME	min	0.6	4.9	101.3					1.43
<i>g+tg+</i>	PFDME	min	115.0	14.6	115.0	7.50	6.96	6.42	4.85	
<i>g+tg+</i>	DME	min	97.1	6.2	97.2					3.13
<i>g+tg-</i>	PFDME	min	113.5	0.0	-113.5		7.28		5.48	
<i>g+tg-</i>	DME	min	93.2	0.0	-93.1					3.08
<i>t+g+g+</i>	PFDME	min	18.5	128.4	116.6	3.40	3.27	2.76	2.01	
<i>t+g-g-</i>	PFDME	min	13.1 ^d	-123.5	-111.3	3.60		2.86		
<i>tg+g+</i>	DME	min	0.7	118.3	112.0					1.51
<i>t+g-g-</i>	PFDME	min	19.5	113.0	-108.1	2.85	3.51	2.79	1.92	
<i>t+g-g+</i>	PFDME	min	13.3 ^d	-118.6	100.2	2.91		2.72		
<i>tg-g-</i>	DME	min	0.9	104.9	-95.8					0.23

^a Alkyl ether entries are italicized. ^b Perfluoroalkyl ether geometries are from D95+* SCF optimizations, except where indicated. Alkyl ether geometries are from D95** SCF optimizations. ^c Energies are relative to the *t+tt+* conformer of PFDME or the *ttt* conformer of DME. ^d Geometries are from 4-31G SCF optimizations.

by examining Figure 2. For the *t+t+* PFDEE conformer, the fluorine-fluorine distances indicated in the figure are quite similar to those found for the same conformation in perfluoroalkanes, and the trans conformation is seen to split as in perfluoroalkanes. The *t+g+* PFDEE conformer, however, is significantly more sterically crowded than the same conformer in perfluoroalkanes, due to the shorter C-O bond lengths. For example, the 1,4 C-C distance in the *g+* conformation in perfluoroalkanes is about 3.3 Å, while the same distance for the C-C-O-C *g+* conformation in PFDEE is only 3.1 Å. The high strain of this conformation is indicated by the much larger C-O-C and O-C-C bond angles in the *t+g+* PFDEE conformer relative to the *t+t+* conformer. The high degree of steric crowding precludes relief of the close fluorine-fluorine and fluorine-carbon interactions by distortion of the gauche torsional angle and results in a significantly higher energy for the C-C-O-C gauche conformation in PFDEE when compared to the C-C-C-C gauche conformation in perfluoroalkanes and the C-C-O-C gauche conformation of DEE (see Table 2). The *t+g-* conformer does not exist in PFDEE because of severe 1,4 CF₂-CF₃ steric interactions. Finally, the *g+g+* conformation in PFDEE is high in energy due to the high energy of the C-C-O-C gauche conformation, while the *g+g-* conformer does not exist due to steric crowding.

Perfluoro-1,2-dimethoxyethane (PFDME). The conformational energies and geometries of the important conformations of PFDME are given in Table 3. As was found for PFDEE, the C-C-O-C trans conformation splits into *t+* and *t-* conformations, while the gauche conformation does not split. No splitting of O-C-C-O conformations in PFDME is seen. The conformations of this bond do not split because of the lack of fluorine substituents on the oxygen atoms; i.e., there are not strong steric interactions to effect distortion of the O-C-C-O bond.

In DME,⁶ the *ttt*, *tgt*, and *tg+g-* conformations were found to be of similar energy, with the *ttt* conformer being the lowest energy conformer by about 0.1–0.2

kcal/mol. In PFDME, the *t+g+t+*, *t+g-t+*, and *t+g+t-* conformers are 0.2–0.3 kcal/mol lower in energy than the *t+tt+* and *t+tt-* conformers. This result indicates that the oxygen gauche effect, which stabilizes the gauche conformation of a bond covalently bonded to oxygen, is also present in perfluoroethers. The oxygen gauche effect is present in DME but is overwhelmed by the strength of the 1,4 O-O electrostatic repulsion in the O-C-C-O gauche conformation.¹² While the O-C-C-O gauche conformation in PFDME results in similar 1,4 O-O electrostatic repulsion, it also results in the relief of 1,4 O-F electrostatic repulsion which occurs in the O-C-C-O trans conformation. As a net result, the O-C-C-O gauche conformation is relatively more favorable in PFDME than in DME.

The fact that PFDME *t+g+t+*, *t+g-t+*, and *t+g+t-* conformers are essentially isoenergetic implies that there is no important coupling between the sense of the distortion of the split trans for the C-O-C-C bond and the conformation of the O-C-C-O bond in PFDME, nor is there coupling between C-O-C-C and C-C-O-C bonds across the O-C-C-O bond. This latter point is also supported by the fact that the *t+tt+* and *t+tt-* conformers are of nearly the same energy. As in PFDEE, the C-C-O-C gauche conformation is high in energy for the PFDME conformers. Because of this high energy and the lack of a 1,5 CH-O electrostatic attraction, the *t+g+g-* conformer in PFDME is much higher in relative energy than the analogous *tg+g-* DME conformer, which was found to be quite low in energy.⁶

Rotational Isomeric State Model for PFPOE

The energies of the conformations of the model molecules given in Tables 2 and 3 were represented in the rotational isomeric state (RIS) approximation as the sum of first-order (depending on the conformation of a single bond) and second-order (depending on the conformation of a bond pair) interactions. The resulting first-order and second-order interactions, with their associated energies, are listed in Table 4. The energies

Table 4. RIS Interactions and Energies in PFPOE Model Molecules

conf	molecule	label	energy ^a	
			PFPOE	POE ^b
First-Order Interactions				
O-C-C-O g^+	PFDME	σ_1	$E_{\sigma_1} = -0.2$	0.1
C-O-C-C g^+	PFDME	σ_2	$E_{\sigma_2} = 2.5$	1.4
Second-Order Interactions				
C-O-C-C-O g^+g^+	PFDME	ψ_1	$E_{\psi_1} = -0.3$	0.0
C-O-C-C-O g^+g^-	PFDME	ω_1	$E_{\omega_1} = -0.4$	-1.3
C-C-O-C-C g^+g^-	PFDEE	ω_2	$E_{\omega_2} = \infty$	1.3

^a Energies are in kcal/mol. ^b For the analogous interaction in the RIS model for POE from ref 12.

Table 5. PFDME and PFDEE RIS Representations

conf	RIS representation	ab initio energy, ^a kcal/mol	RIS energy, ^b kcal/mol
PFDME			
t_+tt_+	0	0.0	0.0
t_+tt_-	0	0.0	0.0
$t_+g^+t_+$	E_{σ_1}	-0.2	-0.2
$t_+g^-t_+$	E_{σ_1}	-0.3	-0.2
$t_+g^+t_-$	E_{σ_1}	-0.3	-0.2
g^+tg^+	$2E_{\sigma_2}$	4.9	5.0
g^+tg^-	$2E_{\sigma_2}$	5.5	5.0
$t_+g^+g^+$	$E_{\sigma_1} + E_{\sigma_2} + E_{\psi_1}$	2.0	2.0
$t_+g^+g^-$	$E_{\sigma_1} + E_{\sigma_2} + E_{\omega_1}$	1.9	1.9
PFDEE			
t_+t_+	0	0.0	0.0
t_+g^+	E_{σ_2}	2.5	2.5
g^+g^-	$2E_{\sigma_2} + E_{\omega_2}$	high	∞

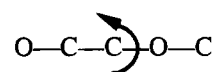
^a Energies are D95+* MP2 values, relative to the PFDME t_+tt_+ conformer or PFDEE t_+t_+ conformer. ^b From first- and second-order RIS energies given in Table 4.

determined for the same interactions in alkyl ether analogs from our previous work are also given in Table 4.

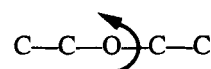
The RIS representations of the conformations of PFDME and PFDEE are given in Table 5. From the PFDME conformer energies we obtain an energy for the O-C-C-O gauche conformation of $E_{\sigma_1} = -0.2$ kcal/mol, indicative of the presence of the oxygen gauche effect in PFE's. For the C-O-C-C bond in PFDEE and PFDME we obtain a relatively high gauche energy of $E_{\sigma_2} = 2.5$ kcal/mol. A small attractive second-order effect is seen for the C-O-C-C-O g^+g^+ conformation, with an energy E_{ψ_1} of about -0.3 kcal/mol. The C-O-C-C-O g^+g^- pairing is also slightly favored, with a second-order energy E_{ω_1} of approximately -0.4 kcal/mol, reflecting the relatively small size of the oxygen atom. As the PFDEE g^+g^- conformer does not exist due to a strong 1,5 second-order repulsion between the large CF₃ groups in the C-C-O-C-C sequence, the second-order energy $E_{\omega_2} = \infty$. The resulting RIS energies for the PFDME and PFDEE conformers are in good agreement with ab initio values, as indicated in Table 5.

Statistical Weight Matrices. From the RIS representations of the conformational energies of the model PFE's given in Table 5, it is possible to construct statistical weight matrices for PFPOE. The three statistical weight matrices required to describe all possible torsional pairs in these polymers are shown in Figure 3. A statistical weight for each first-order or second-order interaction ϕ_i defined in Table 4 is given as

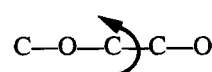
$$\phi_i = f_{\phi_i} \exp(-E_{\phi_i}/kT) \quad (1)$$

Matrix 1

	t_+	t	t_-	g^+	g^+	g^+	g^-	g^-	g^+
t_+	0	0	0	0	0	0	0	0	0
t	1	0	1	0	σ_2	0	0	σ_2	0
t_-	0	0	0	0	0	0	0	0	0
g^+	0	0	0	0	0	0	0	0	0
g^+	1	0	1	0	$\sigma_2\psi_1$	0	0	$\sigma_2\omega_1$	0
g^+	0	0	0	0	0	0	0	0	0
g^-	0	0	0	0	0	0	0	0	0
g^-	1	0	1	0	$\sigma_2\omega_1$	0	0	$\sigma_2\psi_1$	0
g^+	0	0	0	0	0	0	0	0	0

Matrix 2

	t_+	t	t_-	g^+	g^+	g^+	g^-	g^-	g^+
t_+	1	0	0	0	σ_2	0	0	0	0
t	0	0	0	0	0	0	0	0	0
t_-	0	0	1	0	0	0	0	σ_2	0
g^+	0	0	0	0	0	0	0	0	0
g^+	1	0	0	0	0	0	0	0	0
g^+	0	0	0	0	0	0	0	0	0
g^-	0	0	0	0	0	0	0	0	0
g^-	0	0	1	0	0	0	0	0	0
g^+	0	0	0	0	0	0	0	0	0

Matrix 3

	t_+	t	t_-	g^+	g^+	g^+	g^-	g^-	g^+
t_+	0	1	0	0	σ_1	0	0	σ_1	0
t	0	0	0	0	0	0	0	0	0
t_-	0	1	0	0	σ_1	0	0	σ_1	0
g^+	0	0	0	0	0	0	0	0	0
g^+	0	1	0	0	$\sigma_1\psi_1$	0	0	$\sigma_1\omega_1$	0
g^+	0	0	0	0	0	0	0	0	0
g^-	0	0	0	0	0	0	0	0	0
g^-	0	1	0	0	$\sigma_1\omega_1$	0	0	$\sigma_1\psi_1$	0
g^+	0	0	0	0	0	0	0	0	0

Figure 3. Full 9×9 statistical weight matrices for PFPOE.

where E_{ϕ_i} and f_{ϕ_i} are the energies and pre-exponential factors for each interaction. We assume pre-exponential factors of unity for all cases. The statistical weight matrices are 9×9 in order to maintain conformability for all torsional pairs; i.e., both split and nonsplit trans and gauche states must be considered, resulting in nine torsional states. Examination of the statistical weight

Table 6. Geometric Parameters for the RIS Model of PFPOE

bond or angle	bond length or angle	
	PFPOE	POE ^a
C—O	1.36 Å	1.40 Å
C—C	1.55 Å	1.52 Å
C—O—C	122°	115°
O—C—C, C—C—O	108°	111°

torsion angle	rotational isomeric state							
	<i>t</i> ₊	<i>t</i>	<i>t</i> _−	<i>g</i> ⁺ _−	<i>g</i> ⁺	<i>g</i> ⁺ ₊	<i>g</i> [−] _−	<i>g</i> [−] ₊
O—C—C—O—C	19	−19			117			−117
C—C—O—C—C	19	−19			117			−117
C—O—C—C—O		0			119			−119

^a From ref 12.

matrices shows the occurrence of many zero entries, indicating that the conformation of such bond pairs is not allowed. These conformational pairs correspond to conformations of the model molecules which were not energy minima according to the ab initio electronic structure calculations. Some of these conformations are given in Tables 2 and 3.

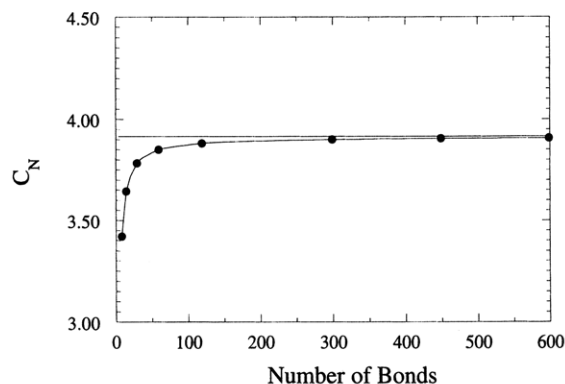
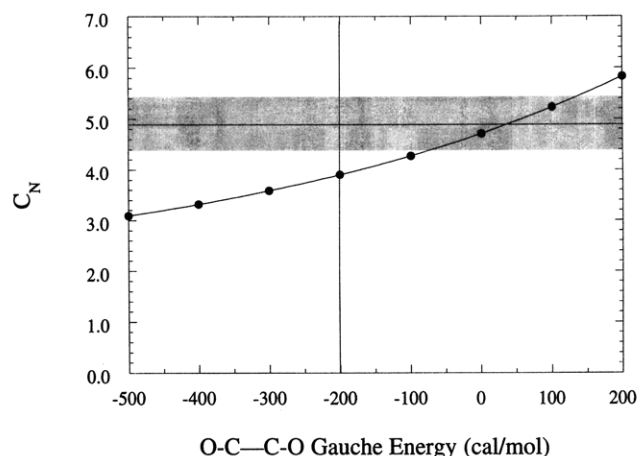
It may be noted that the model described above can be simplified without loss of accuracy in predictions. First, only 5×5 matrices are required to describe PFPOE because the gauche conformations do not split for any bond. In order to be consistent with other PFPE's which we have studied and will be reporting on in future papers, it is convenient to present 9×9 matrices for PFPOE. Second, as is discussed below, the predicted gauche population of the C—O bond in PFPOE is low because of the high value of E_{σ_2} . As a result, assigning statistical weights of unity to ψ_1 and ω_1 (thereby leaving only two energy parameters) has almost no influence on RIS predictions.

Random Coil Dimensions and Conformations of Perfluoropolyethers

Using standard methods, it is possible to calculate the mean-square end-to-end distance of polymer chains within the RIS approximation. The geometric data required for these calculations are given in Table 6, as determined from the ab initio electronic structure calculations. In some cases the torsional angle for a given state was found to depend on the particular conformation, as were the bond angles. In these cases, reasonable averages were taken for the geometric parameters. The dependence of the predicted characteristic ratio on the important geometric parameters is discussed below.

The computed characteristic ratio, $C_n = \langle R^2 \rangle / nl^2$, where $\langle R^2 \rangle$ is the mean-square end-to-end distance, nl^2 is the sum of the bond length squared over all skeletal bonds, and n is the number of bonds, as a function of n , is shown in Figure 4 for PFPOE at 300 K. The high molecular weight value $C_\infty = 3.91$ is also shown. This value, which indicates a very flexible chain, is somewhat lower than the value of 4.9 ± 0.5 obtained from recent viscometric studies,¹ as illustrated in Figure 5.

Dependence on the O—C—C—O Gauche Energy. Parametric studies indicate that the characteristic ratio of PFPOE depends strongly on the energy of the gauche conformation of the O—C—C—O bond, E_{σ_1} , which we have obtained from ab initio quantum chemistry calculations. This dependence is illustrated in Figure 5 for a PFPOE chain of 300 bonds. In order to estimate the uncertainty in E_{σ_1} , we examined the energy of the

**Figure 4.** Predicted characteristic ratio of PFPOE at 300 K as a function of the number of skeletal bonds. The horizontal line indicates the high molecular weight limit.**Figure 5.** Dependence of the characteristic ratio of PFPOE on the O—C—C—O gauche energy for a chain of 300 skeletal bonds at 300 K. The horizontal line indicates the experimental value for a high molecular weight.² The shaded region shows the estimated experimental uncertainty. The vertical line corresponds to our estimate of -0.2 kcal/mol for the gauche energy of the O—C—C—O bond.**Table 7. Influence of Basis Set on PFDME Conformer Energies**

basis set	$E(t_+g^-t_+) - E(t_+tt_+)$ conformer energies	
	SCF	MP2
D95+*	−0.14	−0.31
D95+(2d) ^{a,b}	−0.07	−0.12
D95+(df) ^{a,c}	−0.12	−0.24

^a In these calculations, C atoms are represented by a D95* basis. It was determined that the diffuse functions on C atoms make no significant difference in the relative conformer energies. ^b Polarization exponents were as follows: for C, $\alpha_d = 1.5, 0.375$; for O, $\alpha_d = 1.7, 0.425$; for F, $\alpha_d = 1.8, 0.55$. ^c Polarization exponents were as follows: for C, $\alpha_d = 0.75, \alpha_f = 0.8$; for O, $\alpha_d = 0.85, \alpha_f = 1.4$; for F, $\alpha_d = 0.9, \alpha_f = 1.85$.

$t_+g^-t_+$ conformer of PFDME relative to the t_+tt_+ conformer as a function of the basis set. For this purpose we used the D95+* optimized geometries in determining the conformer energies using D95+*, D95+(2d), and D95+(df) basis sets. These basis sets differ in the number and type of polarization functions. A comparison of relative conformer energies using these basis sets is shown in Table 7. It can be seen that augmenting the polarization functions beyond the minimal representation results in a 0.1–0.2 kcal/mol increase in E_{σ_1} . We conclude that a value of $E_{\sigma_1} = -0.2 \pm 0.3$ kcal/mol is indicated by the ab initio calculations, with E_{σ_1} likely to be somewhat higher than -0.2 kcal/mol due to finite basis set effects. Examination of Figure 5 indicates that

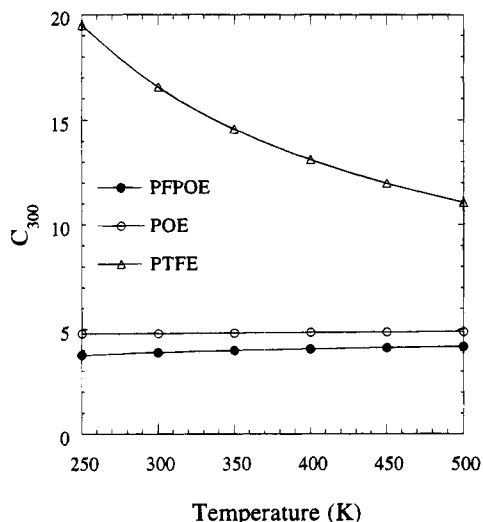


Figure 6. Characteristic ratio of PFPOE, POE, and PTFE as a function of temperature for chains of 300 skeletal bonds.

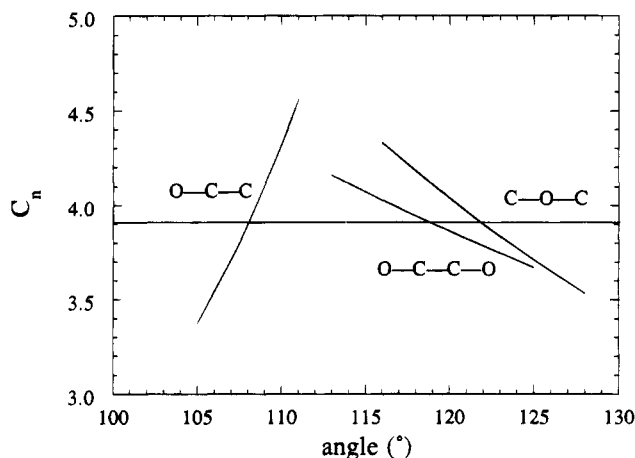


Figure 7. Dependence of the characteristic ratio of PFPOE on the O-C-C and C-O-C valence angles and the O-C-C-O gauche angle for a chain of 300 skeletal bonds at 300 K. Intersections with the horizontal line indicate the average values from ab initio quantum chemistry calculations.

an energy E_{σ_1} somewhat higher than our estimate of -0.2 kcal/mol, but within the estimated uncertainty of about 0.3 kcal/mol, brings the predicted characteristic ratio into good agreement with experiment.

Temperature Dependence. The temperature dependence of the computed characteristic ratio of PFPOE is illustrated in Figure 6, where the computed characteristic ratios of POE and poly(tetrafluoroethylene) (PTFE) are also shown. The characteristic ratios of POE and PTFE were determined using previous RIS models.^{4,12} The characteristic ratio of PFPOE shows a positive temperature dependence, with a value of $d \ln C_n / dT \times 1000$ of about 0.6 at 300 K. The positive temperature dependence is the result of the increase in the trans fraction of the O-C-C-O bond with increasing temperature.

Dependence on Geometric Parameters. The dependence of the characteristic ratio of PFPOE on the O-C-C and C-O-C valence angles and the O-C-C-O gauche angle for a chain of 300 bonds at 300 K, with $E_{\sigma_1} = -0.2$ kcal/mol, is shown in Figure 7. It can be seen that the predicted characteristic ratio of PFPOE is quite sensitive to changes in the valence angles, particularly the O-C-C angle. Because of uncertainties in the ab initio geometries and variations in valence

Table 8. Bond Conformational Populations at 300 K

polymer	bond	population ^a				
		t_+	t	g^{++}	g^+	g^{+-}
PFPOE	C-O-C-C-O		0.26		0.74	
	O-C-C-O-C	0.98			0.02	
	C-C-O-C-C	0.98			0.02	
PTFE	C-C-C-C-C	0.78		0.20		0.02

^a They include both (+ and -) senses of split conformations and gauche states.

and torsional angles between different conformers, we estimated the valence angles to be accurate to about $\pm 2^\circ$ and torsional angles to be accurate to about $\pm 4^\circ$.

Comparison with POE. As can be seen in Figure 6, the predicted characteristic ratio of PFPOE is actually slightly less than that of POE. The small characteristic ratio of POE is due to favorable O-C-C-O-C g^+g^- conformations and a low (but positive) O-C-C-O gauche energy. The small characteristic ratio of PFPOE is a result of both the low O-C-C-O gauche energy and geometric effects. First, the O-C-C-O gauche angle is larger (closer to *cis*) in PFPOE than in POE (119° vs 105°). Second, the O-C-C valence angles are about 3° smaller in PFPOE than POE, as shown in Table 6. Finally, because the C-C-O-C-C sequences in PFPOE are almost entirely $t_{\pm}t_{\pm}$ (see below), while the O-C-C-O bonds are mostly gauche, an increase in the C-O-C valence angle actually leads to a decrease in the predicted characteristic ratio of PFPOE. As shown in Table 6, the C-O-C valence angle in PFPOE is relatively large.

Comparison with PTFE. While PFPOE has a characteristic ratio similar to that of POE, PTFE has a characteristic ratio significantly higher than that of polymethylene. It is apparent that the relationship between the random coil dimensions of a polymer and its perfluorinated analog cannot be simply stated. For perfluoroalkanes (and PTFE), the presence of fluorine atoms results in a splitting of both the trans and gauche conformations of the C-C-C-C bond. The energy of the low-energy gauche state (g^{++}) in perfluoroalkanes was found to be about 0.6 kcal/mol, similar to that of the gauche state in *n*-alkanes. However, the energy of the high-energy gauche state (g^{+-}) was found to be significantly greater, around 2.0 kcal/mol. As a result, at temperatures where the population of g^{+-} states is low, there are essentially two trans (t_+ and t_-) and two gauche (g^{++} and g^{--}) states with significant population for the C-C-C-C bonds, resulting in one populated trans state for every populated gauche state in PTFE. In contrast, there is one populated trans state for the C-C-C-C bond in polymethylene for two gauche states of the bond. Consequently, the gauche fraction of C-C-C-C bonds in PTFE at 300 K is only about 0.22 , while it is 0.39 in polymethylene at the same temperature, resulting in a significant extension of the PTFE chains relative to polymethylene.

The conformational populations of the C-C-O-C, the C-O-C-C, and the O-C-C-O bonds in PFPOE and the C-C-C-C bond in PTFE at 300 K are shown in Table 8. While the C-C-O-C bonds in PFPOE are essentially entirely trans, the O-C-C-O bond shows a high fraction of gauche character. At room temperature, is it possible to think of PFPOE as stiff C-C-O-C-C segments connected by independent, flexible O-C-C-O bonds. At very low temperatures, PFPOE assumes a $\{gt_+t_+\}$ conformation. The trans fraction of the O-C-C-O bond increases with increas-

ing temperature, resulting in a positive temperature dependence of the characteristic ratio at room temperature.

Solvent Effects. The ab initio electronic structure calculations were performed on isolated PFDME and PFDEE molecules; the resulting conformational energies, used in parameterizing the RIS model for PFPOE, do not reflect possible solvent or condensed phase effects which could change the relative conformational energies, and hence chain dimensions. Such condensed phase effects have been observed in DME through both experiment and modeling.¹³ The condensed phase effects in DME have been attributed to a combination of polar effects, which tend to stabilize conformers with large dipole moments such as the *tgt* conformer, in the liquid compared to the gas phase, and a strong intermolecular O \cdots H electrostatic attraction, which competes with 1,5 CH–O intramolecular electrostatic interactions and results in a decrease in the *tg*⁺*g*[–] population in the liquid compared to the gas phase.¹³ For PFDME, and hence PFPOE, we do not expect such interactions to be important. As discussed above, 1,5 CH–O intramolecular electrostatic interactions are not present in the perfluorinated ethers. Unlike DME, dipole moments of PFDME are small for all conformers (<0.2 D). Hence, polar interactions are unlikely to have an important effect on PFDME conformational energies or chain dimensions either in solution or in the melt. The recent experimental studies of the chain dimension of PFPOE² were performed in 1,1,2-trichlorotrifluoroethane, which is both a thermodynamically poor solvent for PFPOE² and relatively nonpolar (we predict a dipole moment of about 0.5 D from ab initio calculations). Therefore, solvent effects are not likely to be important in these experiments and direct comparison with our RIS predictions is valid.

Conclusions

As was seen for the C–C–C–C bond in perfluoroalkanes, the C–C–O–C trans conformation in PFDME and PFDEE splits into *t*₊ and *t*_– conformations in order to alleviate steric crowding. However, steric crowding for the gauche conformation of the C–C–O–C bond in these molecules is so severe as to preclude splitting. The splitting of a bond conformation requires a degree of steric crowding but can be precluded in highly crowded conformations. The O–C–C–O bond does not split in any conformation because there are no fluorine substituents on the oxygen atoms.

In agreement with experiment, our RIS predictions of the characteristic ratio of PFPOE based upon ab initio electronic structure studies of model molecules indicate

a highly flexible chain with a characteristic ratio comparable to or even smaller than that of the alkyl ether analog POE. In contrast, we have found, again in agreement with experiment, that the characteristic ratio of PTFE is much greater than that of its alkyl analog polymethylene. This difference in the behavior of the conformational properties of the polymers on perfluorination is a result of the fact that for the C–C–C–C bond, replacement of hydrogen atoms by fluorine atoms significantly reduces the gauche probability for the bond, while for the O–C–C–O bond, the presence of fluorine atoms increases the gauche probability for the bond.

Acknowledgment. G.D.S. acknowledges the financial support provided by NASA through Eloret Contract NAS2-14031.

References and Notes

- (1) Current address: Department of Chemical Engineering, W2030 Engineering Building East, University of Missouri–Columbia, Columbia, MO 65211.
- (2) Cotts, P. M. *Macromolecules* **1994**, *27*, 6487.
- (3) Chu, B.; Wu, C.; Buck, W. *Macromolecules* **1989**, *22*, 831.
- (4) Smith, G. D.; Jaffe, R. L.; Yoon, D. Y. *Macromolecules* **1994**, *27*, 3166.
- (5) Smith, G. D.; Jaffe, R. L.; Yoon, D. Y. *J. Phys. Chem.* **1993**, *97*, 12752.
- (6) Jaffe, R. L.; Smith, G. D.; Yoon, D. Y. *J. Phys. Chem.* **1993**, *97*, 12745.
- (7) GRADSCF is an ab initio gradient program system designed and written by A. Komornicki at Polyatomics Research Institute, Inc., supported by grants through NASA.
- (8) Dunning, T. H.; Hay, P. J. *Methods of Electronic Structure Theory*; Schaefer, H. F., Eds.; Plenum Press: New York, 1977; pp 1–27.
- (9) Ahlrichs, R.; Bär, M.; Häser, M. H.; Horn, H.; Kölmel, C. *Chem. Phys. Lett.* **1989**, *162*, 165.
- (10) Frisch, M. J.; Head-Gordon, M.; Trucks, G. W.; Foresman, J. B.; Schlegel, H. B.; Raghavachari, K.; Robb, M. A.; Binkley, J. S.; Gonzalez, C.; Defrees, D. J.; Fox, D. J.; Whiteside, R. A.; Seeger, R.; Melius, C. F.; Baker, J.; Martin, R. L.; Kahn, L. R.; Stewart, J. J. P.; Topiol, S.; Pople, J. A. *GAUSSIAN 90 Revision J*; Gaussian, Inc.: Pittsburgh, PA, 1990. Frisch, M. J.; Trucks, G. W.; Head-Gordon, M.; Gill, P. M. W.; Wong, M. W.; Foresman, J. B.; Johnson, B. G.; Schlegel, H. B.; Robb, M. A.; Replogle, E. S.; Gomperts, R.; Andres, J. L.; Raghavachari, K.; Binkley, J. S.; Gonzalez, C.; Martin, R. L.; Fox, D. J.; Defrees, D. J.; Baker, J.; Stewart, J. J. P.; Pople, J. A. *GAUSSIAN 92 Revision E.2*; Gaussian, Inc.: Pittsburgh, PA, 1992.
- (11) Smith, G. D.; Yoon, D. Y.; Jaffe, R. L. *Macromolecules*, in press.
- (12) Smith, G. D.; Jaffe, R. L.; Yoon, D. Y. *Macromolecules* **1993**, *26*, 5216.
- (13) Smith, G. D.; Jaffe, R. L.; Yoon, D. Y. *J. Am. Chem. Soc.* **1995**, *117*, 530.

MA950038+